

Advanced Model-Based Control Studies for the Induction and Maintenance of Intravenous Anaesthesia

Ioana Naşcu, Alexandra Krieger, Clara Mihaela Ionescu, and Efstratios N. Pistikopoulos*

Abstract—This paper describes strategies toward model-based automation of intravenous anaesthesia employing advanced control techniques. In particular, based on a detailed compartmental mathematical model featuring pharmacokinetic and pharmacodynamics information, two alternative model predictive control strategies are presented: a model predictive control strategy, based on online optimization, the extended predictive self-adaptive control and a multiparametric control strategy based on offline optimization, the multiparametric model predictive control. The multiparametric features to account for the effect of nonlinearity and the impact of estimation are also described. The control strategies are tested on a set of 12 virtually generated patient models for the regulation of the depth of anaesthesia by means of the bispectral index (BIS) using Propofol as the administered anaesthetic. The simulations show fast response, suitability of dose, and robustness to induce and maintain the desired BIS setpoint.

Index Terms—Anaesthesia, EPSAC, estimation, interpatient variability, MPC, mp-MPC.

I. INTRODUCTION

ANAESTHESIA plays a very important role in surgery and in the intensive care unit (ICU). It is defined as a reversible pharmacological state of the patient where hypnosis, analgesia, and muscle relaxation are guaranteed [1]. Analgesics block the sensation of pain; hypnotics produce unconsciousness, while muscle relaxants prevent unwanted movement of muscle tone.

The role of the anaesthetist has become more complex and indispensable to maintain the patients' vital functions before, during, and after surgery. To estimate the drug effect in the patient's body and calculate the corresponding drug infusion rates, average population models are used. These strategies may not always be safe for the patient since they do not take into account

any measured variable in a feedback control scheme and even if they reach the desired level of sedation fast, it can result in unsafe minimal values (undershoot) [1]. In stress situations, the anaesthetist has to deal with routine assessments and simultaneously solve complex problems quickly. The automation of some routine actions of the anaesthetist can reduce the workload and consequently increase the safety of the patient.

The control of anaesthesia poses a manifold of challenges: Inter- and intra-patient variability, multivariable characteristics, variable time delays, dynamics dependent on the hypnotic agent, model analysis variability, and agent and stability issues [2], [3]. Hitherto, many PID tuning techniques have been elaborated. Since these classical controllers have no prior knowledge of the drug metabolism, they cannot anticipate the response of the patient and their performance may be suboptimal. Other authors developed model-based strategies using fuzzy [4], predictive [5]–[7], robust [8], [9], adaptive [2], [10], and multiparametric MPC [11] control algorithms and applied them in clinical trials.

Drugs given for the induction and maintenance of depth of anaesthesia (DOA) can be either inhalational or intravenous anaesthetics. An individualized physiological-based, patient specific, compartmental model for volatile anaesthesia is presented and developed in [12] and a combined strategy of model predictive control (MPC) and estimation under uncertainty is presented in [13]. For intravenous anaesthesia, robustness tests of MPC for DOA using the extended predictive self-adaptive controller (EPSAC) for a single-input single-output (SISO) model is presented in [14], different protocols for the administration of Propofol and remifentanyl (multiple-input single-output model) are evaluated in [15], and in [16], a second output variable is determined that originates from the effect of Remifentanyl and leads to the implementation of a MIMO algorithm.

MPC is a model-based control technique that calculates the optimal control action considering constraints on the input, output, and state variables by solving an optimization problem. The downside of this control technique is that the optimization problem has to be solved online. One way to avoid this is to use explicit/multiparametric MPC, which solves offline the optimization problem using multiparametric programming and derives the control inputs as a set of explicit functions of the system states. An important advantage of the multiparametric model predictive control (mp-MPC) is that the previously offline computed control laws can be easily implemented on embedded controllers. These types of devices use programming languages that cannot support powerful mathematical computations.

Manuscript received June 25, 2014; revised September 16, 2014; accepted October 18, 2014. Date of publication October 30, 2014; date of current version February 16, 2015. This work was supported in part by EPSRC under Grant EP/G059071/1 and Grant EP/I014640, the European Research Council (MOBILE, ERC Advanced Grant, No: 226462), and the European Commission (OPTICO/G.A. No. 280813). Asterisk indicates corresponding author.

I. Naşcu and A. Krieger are with the Centre of Process Engineering, Department of Chemical Engineering, Imperial College London, London SW72AZ, U.K. (e-mail: ioana.nascu@imperial.ac.uk; a.krieger@imperial.ac.uk).

C. M. Ionescu is with the Department of Electrical Energy, Systems and Automation, Ghent University, 9052, Gent, Belgium (e-mail: ClaraMihaela.Ionescu@UGent.be).

*E. N. Pistikopoulos is with the Centre of Process Engineering, Department of Chemical Engineering, Imperial College London, London SW72AZ, U.K., and also with the Artie McFerrin Department of Chemical Engineering, Texas A&M University College Station, TX 77843 USA (e-mail: e.pistikopoulos@imperial.ac.uk).

Digital Object Identifier 10.1109/TBME.2014.2365726

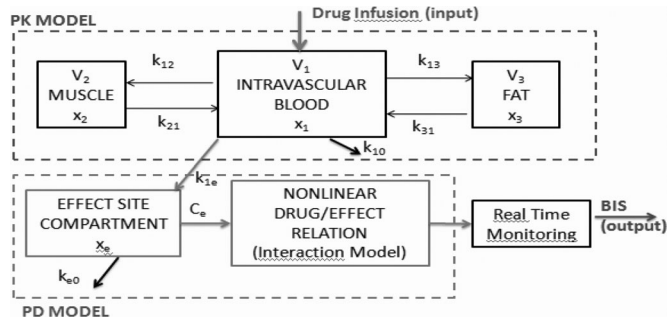


Fig. 1. Compartmental model of the patient, where PK denotes the pharmacokinetic model and PD denotes the pharmacodynamic model.

The optimal control laws are retrievable immediately through simple function evaluations.

The aim of this paper is to design and compare four different types of model-based controllers for administration of Propofol during ICU sedation. Based on a compartmental pharmacokinetic (PK) and pharmacodynamic (PD) patient model, a predictive controller is first designed using an EPSAC strategy and three predictive controllers are designed using an mp-MPC strategy. The difference between the three controllers based on the mp-MPC strategy is that one of them uses the linearized patient model, whereas the other two use the compensation of the nonlinear part of the patient model. In one of the two controllers using the nonlinear compensation, the states are estimated using an online estimator, while for the other one, the states are computed using the nominal patient model.

This paper is organized as follows: The patient model, the multiparametric control strategy, the EPSAC strategy, and the design of the controllers are presented in the following section. Section III presents the simulation results for the induction and maintenance phase and discussions are presented in Section IV. Finally, Section V summarizes the main outcome of this paper.

II. THEORETICAL BACKGROUND

A. Patient Model

A compartmental model is used to describe the PK–PD blocks representing the distribution of drugs in the body, i.e., mass balance. The PK model represents the relation between the drug administration and drug concentration in the body, whereas the PD model represents the relation between the concentration of the drug in the central compartment and the effect observed on the patient. In each compartment, the drug concentration is assumed to be uniform, as perfect and instantaneous mixing is assumed. The structure of the compartmental model is depicted in Fig. 1 [10], [14], [17], [18].

The PK–PD models most commonly used for Propofol are the fourth-order compartmental model described by Schnider [18], [19] and Minto [20], [21], respectively. These models, developed, tested, and validated on a wide range of real patient data are commonly used in the literature for the control of anaesthesia.

PK describes the distribution of the drug in the human body. The PK model and the first term of the PD model are considered

linear studied on real patient data with the collaboration of anaesthesiologists and validated using blood samples provided by hospitals [18], [19], [22]

$$\begin{aligned}\dot{x}_1(t) &= -[k_{10} + k_{12} + k_{13}] \cdot x_1(t) + k_{21} \cdot x_2(t) \\ &\quad + k_{31} \cdot x_3(t) + u(t)/V_1 \\ \dot{x}_2(t) &= k_{12} \cdot x_1(t) - k_{21} \cdot x_2(t) \\ \dot{x}_3(t) &= k_{13} \cdot x_1(t) - k_{31} \cdot x_3(t) \\ \dot{x}_e(t) &= -k_{e0} \cdot x_e(t) + k_{1e} \cdot x_1(t)\end{aligned}\quad (1)$$

where x_1 represents the drug concentration in the central compartment [mg/L]. The peripheral compartments 2 (muscle) and 3 (fat) model the drug exchange of the blood with well and poorly diffused body tissues. The concentrations of drug in the fast and slow equilibrating peripheral compartments are denoted by x_2 and x_3 , respectively. The parameters k_{ij} for $i \neq j$, denote the drug transfer frequency from the i th to the j th compartment, and $u(t)$ [mg/min] is the infusion rate of the anaesthetic or analgesic drug into the central compartment. The parameters k_{ij} of the PK models depend on age, weight, height, and gender and can be calculated for Propofol

$$\begin{aligned}V_1 &= 4.27[l], V_2 = 18.9 - 0.391 \cdot (\text{age} - 53)[l], V_3 = 2.38[l] \\ C_{l1} &= 1.89 + 0.456(\text{weight} - 77) - 0.0681(\text{lbm} - 59) \\ &\quad + 0.264(\text{height} - 177)[l/\text{min}] \\ C_{l2} &= 1.29 - 0.024(\text{age} - 53)[l/\text{min}], C_{l3} = 0.836[l/\text{min}] \\ k_{10} &= \frac{C_{l1}}{V_1}[\text{min}^{-1}], k_{12} = \frac{C_{l2}}{V_1}[\text{min}^{-1}], k_{13} = \frac{C_{l3}}{V_1}[\text{min}^{-1}], \\ k_{21} &= \frac{C_{l2}}{V_2}[\text{min}^{-1}], k_{31} = \frac{C_{l3}}{V_3}[\text{min}^{-1}], k_{e0} = 0.456[\text{min}^{-1}]\end{aligned}\quad (2)$$

where C_{l1} is the rate at which the drug is cleared from the body, and C_{l2} and C_{l3} are the rates at which the drug is removed from the central compartment to the other two compartments by distribution.

The lean body mass (lbm) for men (M) and women (F) are calculated by

$$\text{lbm}_M = 1.1 \cdot \text{weight} - 128 \frac{\text{weight}^2}{\text{height}^2}\quad (3)$$

$$\text{lbm}_F = 1.07 \cdot \text{weight} - 148 \frac{\text{weight}^2}{\text{height}^2}.$$

An additional hypothetical effect compartment is added to represent the lag between plasma drug concentration and drug response. The drug concentration in this compartment is represented by x_e , called the *effect-site compartment concentration*. The effect compartment receives drug from the central compartment by a first-order process and it is considered as a virtual additional compartment. Therefore, the drug transfer frequency for Propofol from the central compartment to the effect site-compartment is considered in clinical practice to be equal to the frequency of drug removal from the effect-site compartment $k_{e0} = k_{1e} = 0.456 [\text{min}^{-1}]$ [18], [19], [23]. When considering the drug effect observed on the patient, the bispectral index

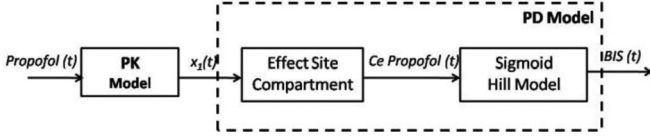


Fig. 2. Schematic representation of the nonlinear SISO patient model for intravenous anaesthesia.

(BIS) variable can be related to the drug effect concentration C_e by the empirical static nonlinear relationship [5], [6], [18], [19], [23], called also the *Hill curve*

$$\text{BIS}(t) = E_0 - E_{\max} \cdot \frac{C_e(t)^\gamma}{C_e(t)^\gamma + \text{EC}_{50}^\gamma}. \quad (4)$$

Notice that in the model used in this paper $C_e = x_e$.

E_0 denotes the baseline value (awake state—without drug), which by convention is typically assigned a value of 100, E_{\max} denotes the maximum effect achieved by the drug infusion, EC_{50} is the drug concentration at 50% of the maximal effect and represents the patient sensitivity to the drug, and γ determines the steepness of the curve.

The inverse of the Hill curve can be defined by the following formulation:

$$C_e(t) = \text{EC}_{50} \left(\frac{E_0 - \text{BIS}(t)}{E_{\max} - E_0 + \text{BIS}(t)} \right)^{\frac{1}{\gamma}}. \quad (5)$$

The type of models that consider a linear dynamic followed by a nonlinear dynamic system are called Wiener-Hammerstein models and are presented in Fig. 2. These type of models have been widely used in control of anaesthesia [23]. For the automatic regulation of DOA in Fig. 2, the anaesthetic agent, i.e., Propofol, is the input and the BIS the output of the system. Because of its pharmacological profile, Propofol is applicable for both induction and maintenance of hypnosis during anaesthesia and intensive care sedation [24].

The BIS is a signal that is derived from the electroencephalogram (EEG) used to assess the level of consciousness in anaesthesia. A BIS value of 0 equals EEG silence, while a BIS value of 100 is the expected value of a fully conscious adult patient, 60–70 and 40–60 range represents light and moderate hypnotic conditions, respectively. The target value during surgery is 50, giving us a gap between 40 and 60 to guarantee adequate sedation [1]–[3].

B. Advanced Model-Based Control Strategies

MPC is a control methodology based on two main principles: explicit online use of a *process model* to *predict* the process output at future time instants, and the computation of an optimal control action by minimizing one or more *cost functions*, including *constraints* on the process variables.

The main differences between the different types of MPC algorithms are: the *type of model* used to represent the process and its *disturbances* and the *cost function(s)* to be minimized, with or without *constraints*.

1) *EPSAC Strategy*: For the EPSAC approach, described in detail in [25], the controller output is obtained by minimizing

the cost function

$$\sum_{k=N_1}^{N_2} [r(t+k/t) - y(t+k/t)]^2 + \lambda \sum_{k=0}^{N_u-1} [\Delta u(t+k/t)]^2. \quad (6)$$

The design parameters are: N_1 = the minimum costing horizon, N_2 = the maximum costing horizon, $N_2 - N_1$ = the prediction horizon, N_u = control horizon, λ = weight parameter, $n(t)$ is the disturbance, $y(t)$ the measured output, and $u(t)$ the model input. The signal r represents the *reference trajectory*.

In our case, the process input is represented by the Propofol infusion rate applied to the patient. The process output is predicted at time instant t over the prediction horizon $N_2 - N_1$, based on the measurements available at that moment and the future outputs of the control signal. The cost function is an extended EPSAC cost function that penalizes the control movements using the weight parameter λ .

2) *Multiparametric Strategy*: Multiparametric programming is a technique to solve an optimization problem, where the objective is to minimize or maximize a performance criterion subject to a given set of constraints where some of the parameters vary between specified lower and upper bounds. The main characteristic of the mp-MPC is its ability to obtain: 1) the objective and optimization variable as a function of the varying parameters, and 2) the regions in the space of the parameters where these functions are valid [critical regions (CR)] [26], [27]. This reduces the online implementation of the MPC to simple function evaluation, facilitating real-time applications.

For the mp-MPC, the generic optimization problem solved is

$$\begin{aligned} \min_{x,y,u} J = & x_N' P x_N + \sum_{k=1}^{N-1} x_k' Q_k x_k \\ & + \sum_{k=1}^{N-1} (y_k - y_k^R)' Q R_k (y_k - y_k^R) \\ & + \sum_{k=0}^{N_u-1} (u_k - u^R)' R_k (u_k - u^R) \\ & + \sum_{k=0}^{N_u-1} \Delta u_k' R_{1k} \Delta u_k \\ \text{s.t. } & x_{t+1} = A x_t + B u_t \\ & y_t = C x_t \\ & \text{BIS}_{\min} \leq y \leq \text{BIS}_{\max} \\ & \Delta u_{\min} \leq \Delta u \leq \Delta u_{\max} \\ & x_t \in X \subseteq \mathbb{R}^p, \quad u_t \in U \subseteq \mathbb{R}^s \end{aligned} \quad (7)$$

where x are states, y are outputs, and u are controls, all (discrete) time-dependent vectors. The subsets of output variables that get tracked have time-dependent set points y^R . Finally, Δu are changes in control variables, $\Delta u(k) = u(k) - u(k-1)$. The prediction horizon is denoted by N and control horizon by N_u . X and U are the sets of the state and input constraints that

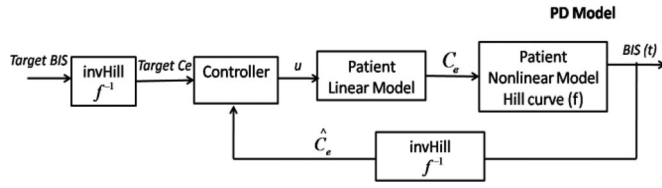


Fig. 3. MPC control scheme.

contain the origin in their interior. Both $Q > 0$, the objective coefficient for the states and $P > 0$, the terminal weight matrix for the states, are symmetric semipositive definite matrices. The quadratic matrix for manipulated variables $R > 0$ is a symmetric positive matrix, QR is the quadratic matrix for tracked outputs, and $R1$ is a weight matrix for the control action changes (Δu). The control problem is posed as a quadratic convex optimization problem for which an explicit solution can be obtained as follows:

$$u = f(x) = \begin{cases} K_1 x + c_1, & \text{if } x \in \text{CR}^1 \\ \dots & \\ K_s x + c_s, & \text{if } x \in \text{CR}^s \end{cases} \quad (8)$$

where s is the number of CR.

C. Control Design

The presence of the Hill nonlinearity complicates the use of linear controller synthesis. Two methods to overcome this problem have been proposed: Exact and local linearization. Exact linearization is based on the compensation of the nonlinearity introduced by the Hill curve, in the PD model. Since the Hill nonlinearity (4) is a monotonic function (f) of the normalized effect site concentration, it has an inverse presented in (5). Using a parameter scheduling technique, the inverse Hill function (f^{-1}) could be implemented in the controller as illustrated by the block diagram in Fig. 3. Here, f is using the nonlinearity parameter of the real patient ($E_0, E_{\max}, EC_{50}, \gamma$), while f^{-1} is using the parameter assumed by the controller (the nominal patient nonlinearity parameters *a priori* known ($E_0^{\text{mean}}, E_{\max}^{\text{mean}}, EC_{50}^{\text{mean}}, \gamma^{\text{mean}}$). The controller aims at controlling the estimated drug concentration \hat{C}_e , which is straight-forward, using a linear controller.

An exact linearization occurs only in the case where the patient model is identical to the nominal model in which case it completely cancels the nonlinearity and $\hat{C}_e = C_e$. The local linearization is based on the linearized PK-PD model for a BIS value of 50 obtained using gPROMS [28].

An important challenge of DOA control is the high inter- and intra-patient variability. This results in different dynamics in PK model, and changes in the parameters of the Hill function for each patient model. Four control strategies, a model predictive controller, EPSAC, and three different mp-MPC are designed and evaluated. The framework for the different ways of designing the controllers is presented in Fig. 4.

The patient response is simulated using patient model block, composed of the PK-PD linear part (1) and the nonlinear PD part, the Hill nonlinearity (4). BIS can be measured; however,

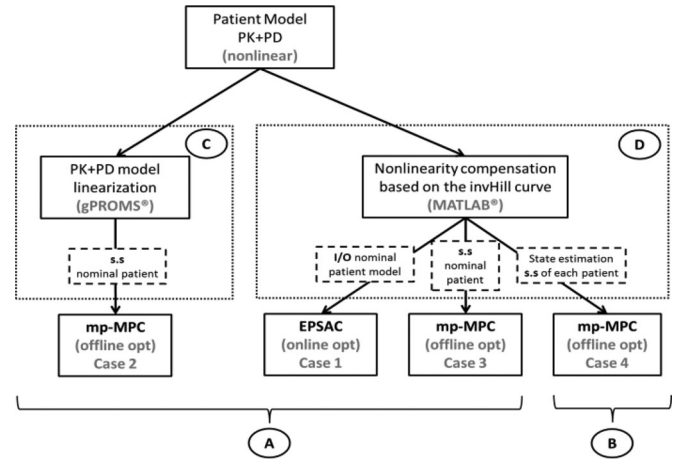


Fig. 4. Control scheme development flowchart.

the states cannot and have to be estimated: either using the drug rate and the nominal state-space patient model or by using the input and output measured output (BIS) of the process, the state-space nominal model and a correction estimator based on the output changes.

To analyse the influence of the changes in the dynamics of the PK model on the control performances, two types of control schemes are implemented, one uses the states given by the nominal model (B) and the other uses an estimator to adjust the states based on the dynamics of each patient (A).

The influence to the changes of parameters of the Hill curve on the control performances is analyzed by two types of control schemes, one using the local linearized PK-PD model (C) and the second is based on the exact linearization (D). The following design parameters are used: The objective coefficients for states (x), $Q = 0$, when we have no state estimation and $Q = 1$ in the case with state estimation, the quadratic matrix for tracked outputs (y), $QR = 1000$, quadratic matrix for manipulated variables (u), $R = 1$, the control horizon $N_u = 1$, and the prediction horizon $N = 20$ in both mp-MPC and EPSAC. The EPSAC has an extra weighting factor λ from (8) for which its default value $\lambda = 0$ was used. The states used in the design of the controllers are x_1, x_2, x_3, x_e as described in (1). The clinically recommended sampling time is of 5 s [6]. N_1, N_2 , and N_u are chosen based on the characteristics of the process and the desired performances. Based on [29], [30], N should be large, at least $2n-1$ but not larger than the risetime of the process. For anaesthesia, due to medical procedures, we are constrained to use a small sampling time leads to a choice of a greater value for N . Also, the dead time is not considered since it is very small and does not affect the process, therefore $N_1 = 1$. In choosing N_u for processes with no unstable/underdamped poles, like anaesthesia, $N_u = 1$ is generally satisfactory. A choice of the Q, R , and QR is given by Bryson's rule [31].

1) *Case 1: Extended Prediction Self-Adaptive Control:* In this section, we apply a particular case of online MPC, the EPSAC strategy described in detail in Section II-C. The structure of the control system proposed in this section is shown in Fig. 5.

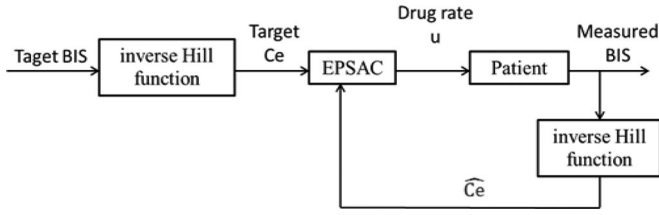


Fig. 5. Case 1: EPSAC control scheme.

TABLE I
BIOMETRIC VALUES OF THE VIRTUAL PATIENTS

Patient	Age	Height (cm)	Weight (Kg)	Gender	EC ₅₀	E ₀	γ
1	40	163	54	M	6.33	98.8	2.24
2	36	163	50	M	6.76	98.6	4.29
3	28	164	52	M	8.44	91.2	4.1
4	50	163	83	M	6.44	95.9	2.18
5	28	164	60	F	4.93	94.7	2.46
6	43	163	59	M	12.0	90.2	2.42
7	37	187	75	F	8.02	92.0	2.1
8	38	174	80	M	6.56	95.5	4.12
9	41	170	70	M	6.15	89.2	6.89
10	37	167	58	M	13.7	83.1	1.65
11	42	179	78	F	4.82	91.8	1.85
12	34	172	58	M	4.95	96.2	1.84
Mean	38	169	65	M	7.42	93.1	3

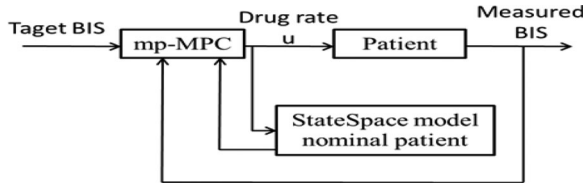


Fig. 6. Case 2: mp-MPC without nonlinearity compensation control scheme.

The patient block is composed of the PK and PD models. Control strategy based on nonlinearity compensation and I/O linear nominal patient model is used (see Fig. 4). The controller output is obtained by minimizing cost function (6) with the design parameters in Section II-B1. The control algorithm uses for prediction a transfer function derived from the PK-PD linear model (1). The inverse of the Hill curve (5) is used to compensate the nonlinearity. Both the linear model and the inverse of the Hill curve use the nominal values from Table I.

2) *Case 2: mp-MPC Without Nonlinearity Compensation:* The structure of the control scheme is presented in Fig. 6. This approach uses the explicit/multiparametric MPC strategy based on local linearization of the PK-PD model and the state-space model of the linearized nominal patient model (see Fig. 4).

To obtain the linearized patient model, we will first implement the PK and PD model for the nominal patient in gPROMS [28], and determine the state space of the linearized nominal patient model at BIS = 50. Using these matrices, the mp-QP optimization problem (7) is solved to obtain the CR using a MATLAB implementation of multiparametric quadratic programming algorithm [32] and determine the mp-MPC controller.

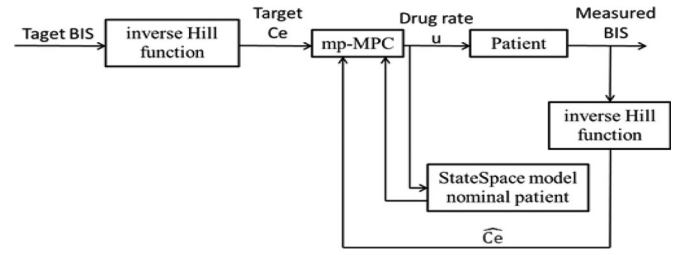


Fig. 7. Case 3: mp-MPC with nonlinearity compensation control scheme.

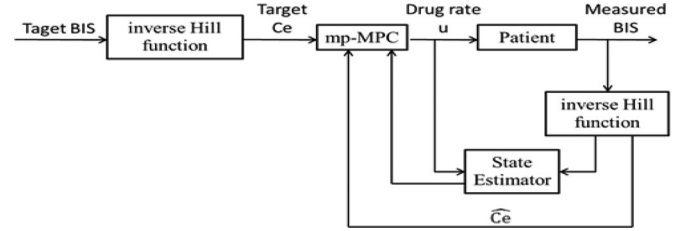


Fig. 8. Case 4: mp-MPC with nonlinearity compensation and estimator control scheme.

3) *Case 3: mp-MPC With Nonlinearity Compensation:* The explicit/multiparametric MPC is used again. Control strategy based on nonlinearity compensation and the state-space model of the PK-PD linear part (1) for the nominal patient model is used (see Fig. 4). The PK-PD model is no longer linearized as a whole in gPROMS like in the previous case (Case 2). Instead, the PK-PD linear part (1) is implemented in MATLAB and is used to obtain the state space of the nominal patient characteristics (A, B, C, and D matrices). Having the state space obtained, we solve the mp-QP optimization problem (7), obtain the CR using POP [32] and determine the controller based on the nominal patient values.

The inverse of the Hill curve (5) based on the nominal patient model parameters is then used to compensate the nonlinearity. Note that the states are obtained using the state-space model based on the A, B, C, and D matrices and the drug rate u as input. This control scheme is presented in Fig. 7.

4) *Case 4: mp-MPC With Nonlinearity Compensation and Estimation:* This approach also uses the explicit/multiparametric MPC strategy. The structure of this control scheme is similar to the one described in Section II-C3 and it is presented in Fig. 8.

The difference is that the state-space model nominal patient block from Fig. 7 is replaced by a state estimator. Here, the real patient states are estimated using a Kalman filter [33] based on the state space of the nominal patient, the online BIS measurement, and the drug rate.

III. RESULTS

In this section, the results of a simulation study to evaluate the four control strategies for the administration of Propofol are presented. DOA is monitored using the BIS during the induction and maintenance phase of general anaesthesia. The closed-loop control tests are performed on a set of 12 patients [14] plus an

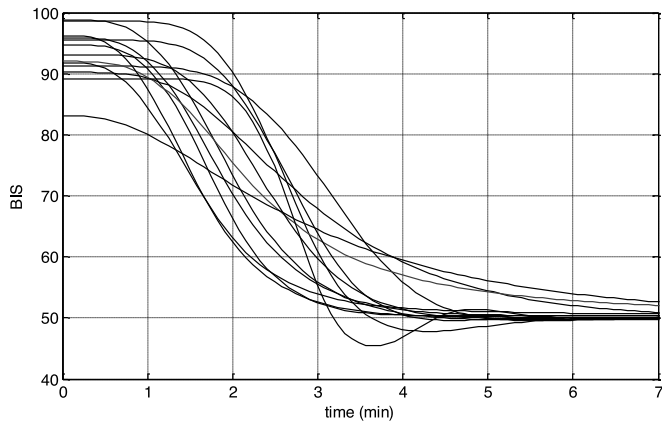


Fig. 9. BIS output for all 13 patients for Case 1.

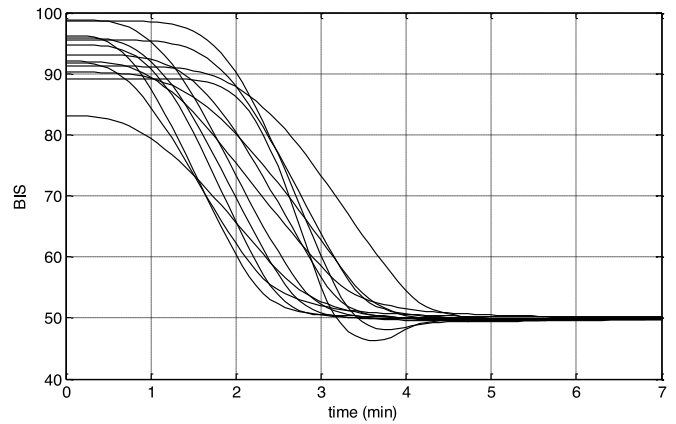


Fig. 11. BIS output for all 13 patients for Case 2.

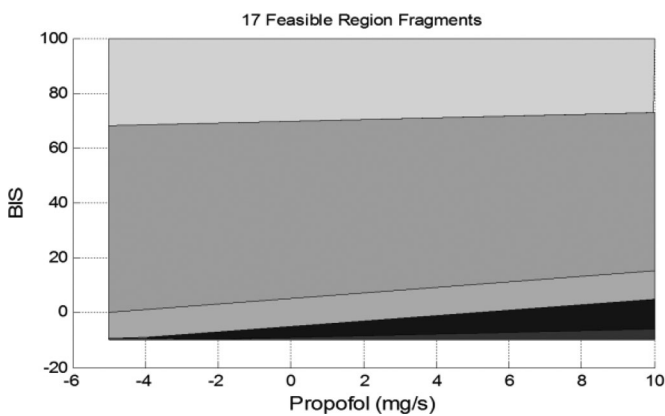


Fig. 10. Map of CR: Case 2.

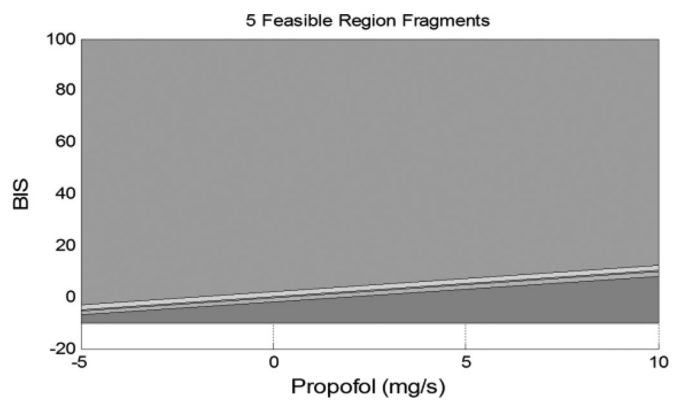


Fig. 12. Map of CR: Case 3 and Case 4.

extra patient representing the nominal values of all 12 patients (PaN—patient nominal). The parameters values of these patients are given in Table I and are also used to calculate the parameters of the patient model.

All designed controllers are simulated first for the set of data presented in Table I in order to have a better understanding of their behavior on the different types of patients, and analyze the inter- and intra-patient variability. Next, the four controllers will be tested against each other and simulated for different patients so as to be able to compare their performances by means of the BIS index and the corresponding Propofol infusion rates.

A. Induction Phase

Ideally, the induction phase of the patient in an operational DOA is performed as fast as possible, such that little time is lost before the surgeon can start operating. It is, therefore, desirable that the patient reaches the $BIS = 50$ target and remains within the target value without much undershoot or overshoot, i.e., values below $BIS = 40$ and above $BIS = 60$ should be avoided. In Figs. 9, 11, 13, and 14, we have the simulations of the four controllers for all 12 patients and the nominal one in the induction phase. Fig. 10 presents the map of the CR for the controller using local linearization (Case 2); and in , we have the map of

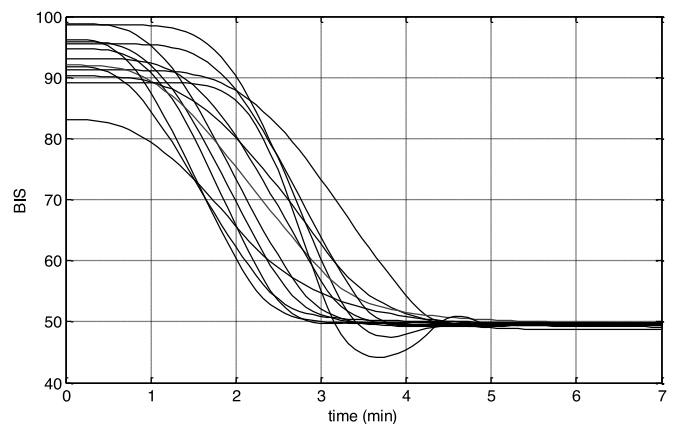


Fig. 13. BIS output for all 13 patients for Case 3.

the CR for the controllers designed using exact linearization, by using the inverse of the Hill curve (Cases 3 and 4).

Simulations of some patients show very small oscillations around the steady-state values. The average settling time for EP-SAC is approximately 7 min, and for the mp-MPC controllers is approximately 5 min. In common practice, the operation procedure does not start until the patient reaches an adequate DOA,

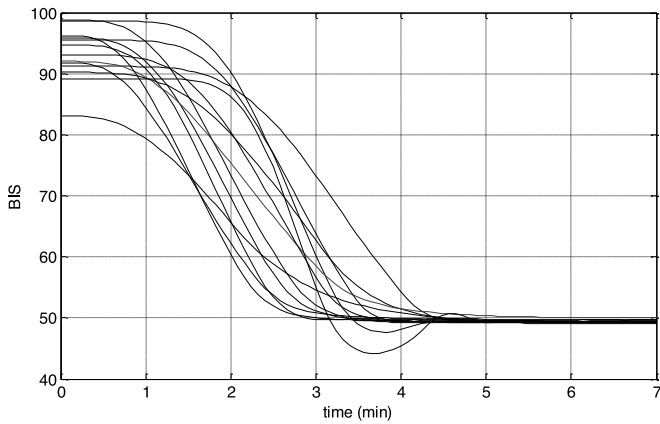


Fig. 14. BIS output for all 13 patients for Case 4.

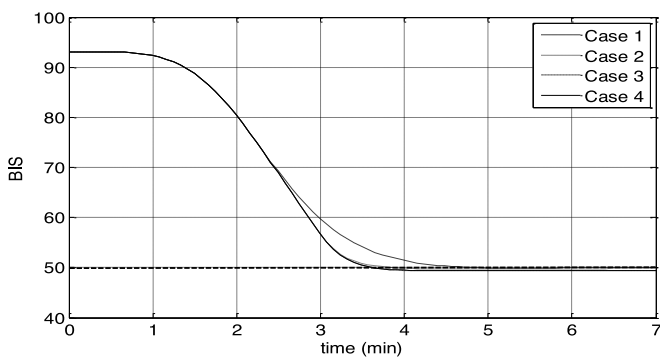


Fig. 15. BIS response for the four controllers for PaN.

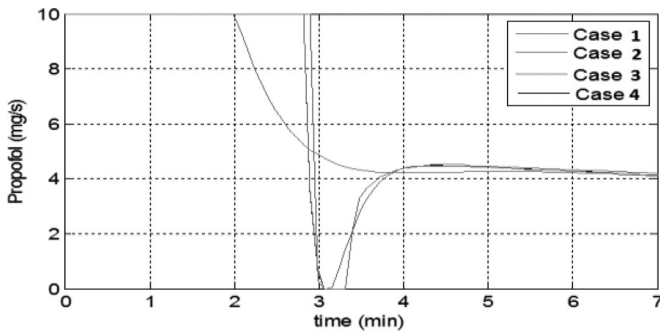


Fig. 16. Output for the four controllers for the PaN.

usually taking up to 15 min. Thus, a risetime between 5 and 7 min gives good performances.

The best performances are obtained for Case 2. It seems that the local linearization is able to deal with inter- and intra-patient variability. Also, the process was linearized at $BIS = 50$, which is the value of the controller set point. The EPSAC controller is more influenced by interpatient variability and for some patients the settling time has greater values.

The four controllers: EPSAC and the mp-MPC controllers, are simulated, compared for PaN and presented in Fig. 15. For patient 9, the most sensitive patient, this simulation is presented in Fig. 17. In Figs. 16 and 18, we have the corresponding Propo-

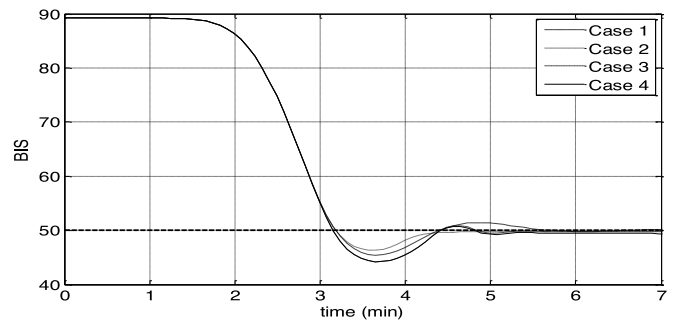


Fig. 17. BIS response for the four controllers for patient 9.

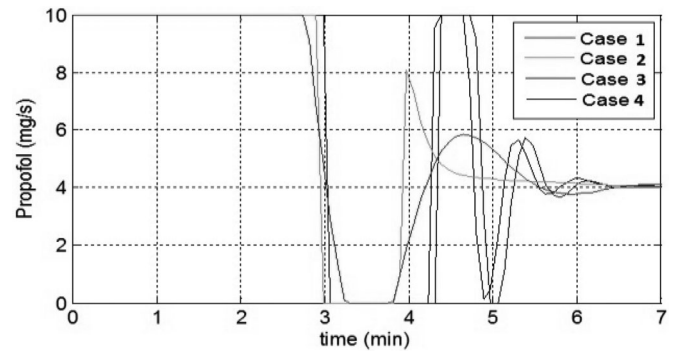


Fig. 18. Output for the four controllers for patient 9.

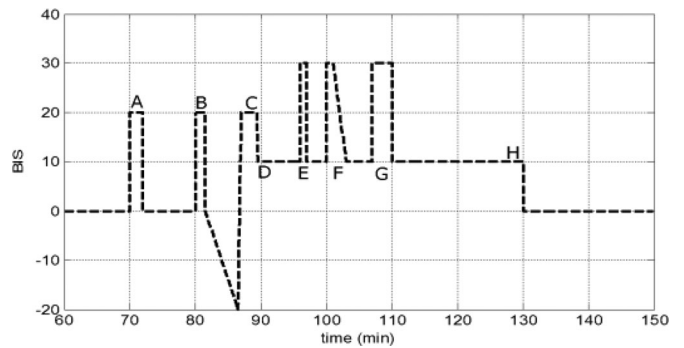


Fig. 19. Artificially generated disturbance signal.

fol infusion rates for the two patients. We can observe that due to the less aggressive behavior of the EPSAC controller, the output evolution will be smoother. In all the cases, the Propofol infusion rates are limited to 10 mg/s due to pump restrictions. The same conclusions as for Figs. 9–12 are valid here. For both simulated patients, the EPSAC controller has a slower response.

B. Maintenance Phase

During the maintenance phase, it is important that the controller rejects the disturbances occurred during surgery as fast as possible and bring the patient to the BIS target value. In this phase, typical disturbances can be applied additively to the output of the process to check the controller's ability to reject them [22]. A standard stimulus profile is defined and is presented in

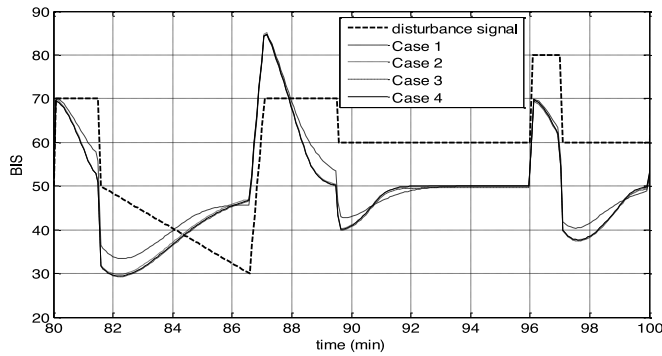


Fig. 20. BIS response for the four controllers for PaN with disturbance.

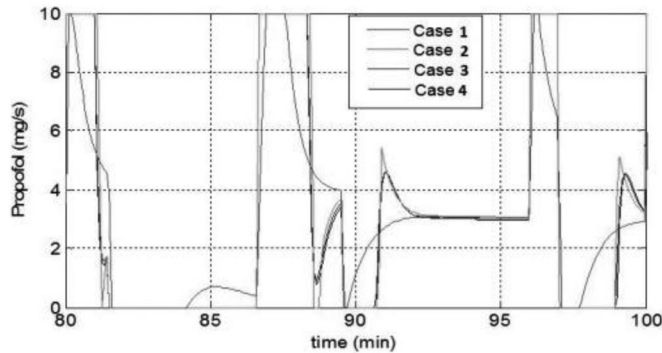


Fig. 21. Output for the four controllers for PaN with disturbance.

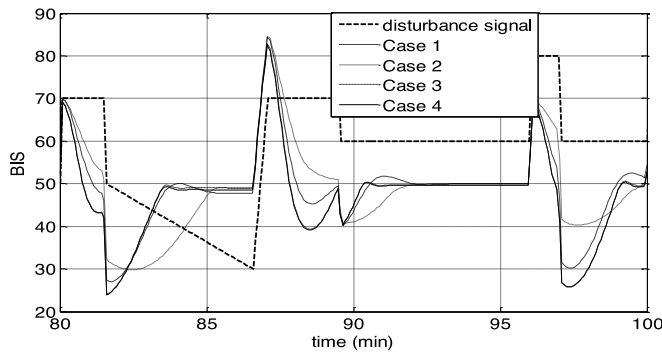


Fig. 22. BIS response for the four controllers for patient 9 with disturbance.

Fig. 17. Each interval denotes a specific event in the operation theatre. Stimulus A represents response to intubation; B represents a surgical incision that is followed by a period of no surgical stimulation (i.e., waiting for pathology result); C mimics an abrupt stimulus after a period of low level stimulation; D represents the onset of a continuous normal surgical stimulation; E, F, and G simulate short-lasting, larger stimulation within the surgical period; and H represents the withdrawal of stimulation during the closing period [34].

In Figs. 20 and 22, the performance of the disturbance rejection of the four controllers for PaN and a more sensitive patient (patient 9) are shown. The figures present the most challenging part of the disturbance rejection test, namely B-C-D-E. In

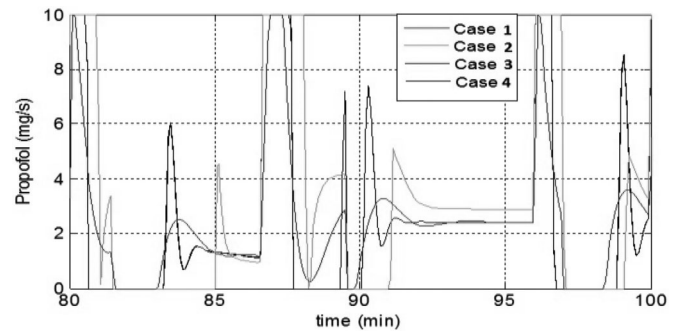


Fig. 23. Output for the four controllers for patient 9 with disturbance.

Figs. 21 and 23, we have the corresponding Propofol infusion rate for PaN and patient 9, limited between 0 and 10 mg/s. The simulations are performed for the maintenance phase using the disturbance signal (see Fig. 19) between 60 and 140 min. The simulations show only small differences between the controllers and, thus, comparable performances of all four controllers. For the second control scheme, the behavior of the controller is less aggressive; the response is slower but it also has the smallest values of the undershoot.

IV. DISCUSSION

The aim of this study is to evaluate the performance of a model-based predictive control algorithm and model predictive multiparametric control for automatic induction and control of DOA during the induction and the maintenance phases.

Some of the most important aspects of this application are the high inter- and intra-patient variability, variable time delays, dynamics dependent on the hypnotic agent, and model analysis variability. These are just some of the issues that are dealt with when trying to control the DOA.

In this paper, the hypnotic agent Propofol is given as the input and the output is described by the BIS, resulting in a SISO system. SISO patient models for control of most anesthetic drugs already exist in the literature and their parameters are estimated based on age, weight, gender, and height.

Four different types of controllers are designed and tested. The first controller is based on the online optimization EPSAC MPC technique. The other three controllers are based on the offline optimization mp-MPC: one uses the linearized patient model and the other two uses the compensation of the nonlinear part of the patient model. The difference between the two control strategies using nonlinearity compensation is that for one of them the states are computed using the nominal patient model, whereas the other one uses an online estimator.

In order to address the issue of inter- and intra-patient variability, each of the four controllers are first tested for the whole set of patients presented in Table I for the induction and the maintenance phase. The maps of the CR for the mp-MPC are presented in Figs. 10 and 12. One can observe that for the controllers using the nonlinearity compensation (exact linearization), there are less CR than for the controller using local linearization. This

will make the controllers from Cases 3 and 4 easier to implement on embedded devices.

In the induction phase, for Case 1, representing the online EPSAC controller, we have an average settling time of 390 sec. The undershoot of the most sensitive patient is of 4.6%. As it can be observed from Figs. 11, 13, and 14, representing the BIS response of the mp-MPC controllers, the three cases have very similar settling time, lower than for the EPSAC strategy, an average of 270 sec. For the undershoot evaluation, the worst-case scenario is considered, meaning the most sensitive patient. We obtain for the first controller (Case 2) an undershoot of 3.7%; for Case 3, an undershoot of 5.8%; and for Case 4, an undershoot of 5.78%. All undershoots are below 10%, which represents the maximum limit. For the induction phase, it can be said that all four controllers perform well each of them having their own advantages: i.e., lower settling time and smaller undershoot.

The controllers are tested in the maintenance phase in order to see how well they can deal with the disturbance rejection. In Figs. 20 and 22, we can observe the four controllers response to a disturbance signal that mimics the events that occur in an operation theatre for PaN and for patient 9.

All four controllers are tested against each other for the induction and maintenance phase for two different patients. The first patient is PaN, and the second patient used for comparison, patient 9, represents the most sensitive patient. It is worth mentioning that the controllers are designed using the values of the nominal patient which means that for this patient, we will have the best behavior of the controllers. As it can be observed from Figs. 15, 16, 20, and 21, the BIS response and the output for PaN in the induction phase and the maintenance phase, respectively, the three offline controllers have a very similar behavior. All the controllers present no undershoot and a fast settling time. The EPSAC controller has a less aggressive behavior; hence, a longer settling time compared to the mp-MPC controllers, but as can be observed in the maintenance phase, it will have less undershoot. In Figs. 17, 18, 22, and 23, we have the BIS response and the output for patient 9 in the induction phase and the maintenance phase. This patient represents the worst-case scenario since it is the most sensitive patient. We can observe from the figures that all four controllers have good performances and their responses are very close to each other. However, the controller from Case 2 gives the best performances for this patient in the induction phase particularly lower undershoot, 3.7%, and faster settling time, 300 sec. This shows that the combination between the linearization method based on gPROMS and optimization methods based on mp-MPC gives good results even without the nonlinearity compensation.

It is important to state that the mp-MPC controller designed using the linearized patient model is the simplest version of the four controllers since it does not use an estimator and it avoids using the nonlinearity compensation, which introduces additional complexity in the DOA control. Moreover, it obtains the best performances which can be explained through the fact that the nonlinearity of the Hill curve is more intense at extreme values of the BIS index and weaker around the BIS value of 50 where the model was linearized and where the BIS target is set. If the induction phase and the maintenance phase are kept around

the value of 50%, Case 2 will give very good performances. But if the disturbances take the process out of the 50% area, we can observe that the performances are not as good as in the case of nonlinearity compensation. Case 2 does not provide good performances if the disturbances are substantial. Due to the Hill nonlinearity, the real-patient model has smaller gain at the extreme values of the control variable. In the case of substantial disturbances, the control variable goes to the extreme values and the controller has a slower response but also a lower undershoot/overshoot.

Using nonlinearity compensation is a good alternative in this case. Moreover, the computations required for the nonlinearity compensation are rather straightforward (the inverse of the Hill curve), and there are no recursive computations that might lead to accumulation of errors.

The estimator used for the mp-MPC with nonlinearity compensation can also be applied for the mp-MPC using local linearization. It was not used for this study because as it can be observed from the simulations, the case with nonlinearity compensation is more meaningful in the presence of disturbance.

The aim of the studies on control of anaesthesia is to be able to implement the controllers on embedded devices (see MOBILE project). These types of devices do not have the same computational power as the computers where simulations are performed in real time. This would make classical MPC more difficult to implement since matrix operations are harder to program on embedded devices. The mp programming algorithms derive the explicit mapping of the optimal control actions as a function of the current states resulting in the implementation of a simple lookup table and simple function evaluations. This makes the mp-MPC controllers much easier to implement for the control of DOA.

For each patient, there will be a variable dose-response relationship. For the same reference value, the controller sends different drug rate and the blood and effect-site concentrations levels are different for each patient. The safety limit for Propofol blood concentration and effect-site concentration is fulfilled by maintaining the drug infusion rate below 10 mg/s. It can be observed from Figs. 16, 18, 21, and 23 that the drug infusion rates are maintained below this limit.

Note that the robustness of the performance is analyzed by having the controllers designed on a nominal model [6] and then tested on a wide set of patient models parameters where the impact of parameter uncertainties were analyzed. Formal robust criteria can also be included [27], and this represents a topic of our ongoing research.

V. CONCLUSION

In this paper, we design and evaluate four different controllers for the regulation of DOA during induction and maintenance phase. For the maintenance phase, a realistic disturbance signal was considered and applied. A simulation study is performed on a set of 12 virtually generated patients plus the mean patient. The performance of the four controllers is compared with each other for a sensitive patient and the nominal patient.

Some important aspects of this application are the high interpatient variability and the presence of important disturbances during the maintenance phase. The results show a high-efficiency, optimal dosage, and robustness of the MPC algorithm to induce and maintain the desired BIS reference while rejecting typical disturbances from surgery. The mp-MPC approach, which is an offline optimisation method, has similar performances with the online method and promising results.

REFERENCES

- [1] J. M. Bailey and W. M. Haddad, "Drug dosing control in clinical pharmacology," *IEEE Control Syst. Mag.*, vol. 25, no. 2, pp. 35–31, Apr. 2005.
- [2] W. M. Haddad, T. Hayakawa, and J. M. Bailey, "Nonlinear adaptive control for intensive care unit sedation and operating room hypnosis," in *Proc. Amer. Control Conf.*, 2003, pp. 1808–1813.
- [3] A. R. Absalom, R. De Keyser, and M. M. R. F. Struys, "Closed loop anaesthesia: Are we getting close to finding the Holy Grail?" *Anesthesia Analgesia*, vol. 112, pp. 516–518, 2011.
- [4] M. Curatolo, M. Derighetti, S. Petersen-Felix, P. Feigenwinter, M. Fischer, and A. M. Zbinden, "Fuzzy logic control of inspired isoflurane and oxygen concentrations using minimal flow anaesthesia," *Brit. J. Anaesthesia*, vol. 76, pp. 245–250, 1996.
- [5] M. M. R. F. Struys, H. Vereecke, A. Moerman, E. W. Jensen, D. Verhaeghen, and N. De Neve, "Ability of the bispectral index, autoregressive modelling with exogenous input-derived auditory evoked potentials, and predicted propofol concentrations to measure patient responsiveness during anaesthesia with propofol and remifentanyl," *Anesthesiology*, vol. 99, pp. 802–812, 2003.
- [6] C. M. Ionescu, R. D. Keyser, B. C. Torricco, T. D. Smet, M. M. R. F. Struys, and J. E. Normey-Rico, "Robust predictive control strategy applied for propofol dosing using BIS as a controlled variable during anaesthesia," *IEEE Trans. Biomed. Eng.*, vol. 55, no. 9, pp. 2161–2170, Sep. 2008.
- [7] R. Hodrea, R. Morar, and I. Nascu, "Predictive control of neuromuscular blockade," *Autom. Comput. Appl. Math.*, vol. 21, pp. 119–205, 2012.
- [8] V. Caiado Daniela, M. Lemos João, and A. Costa Bertinho, "Robust control of depth of anaesthesia based on H_∞ design," *Arch. Control Sci.*, vol. 23, pp. 41–59, 2013.
- [9] G. A. Dumont, A. Martinez, and J. M. Ansermino, "Robust control of depth of anaesthesia," *Int. J. Adapt. Control Signal Process.*, vol. 23, pp. 435–454, 2009.
- [10] I. Nascu, I. Nascu, C. M. Ionescu, and R. De Keyser, "Adaptive EPSAC predictive control of the hypnotic component in anaesthesia," in *Proc. Int. Conf. Automat. Quality, Testing Robot.*, 2012, pp. 103–108.
- [11] I. Nascu, R. S. C. Lambert, A. Krieger, and E. N. Pistikopoulos, "Simultaneous multi-parametric model predictive control and state estimation with application to distillation column and intravenous anaesthesia," *Comput. Aided Chem. Eng.*, vol. 33, pp. 541–546, 2014.
- [12] A. Krieger, N. Panoskaltsis, A. Mantalaris, M. C. Georgiadis, and E. N. Pistikopoulos, "Analysis of an individualized physiologically based model for anaesthesia control," in *Proc. IFAC Symp. Biol., Med. Syst.*, 2012, pp. 385–390.
- [13] A. Krieger, N. Panoskaltsis, A. Mantalaris, M. C. Georgiadis, and E. N. Pistikopoulos, "Modeling and analysis of individualized pharmacokinetics and pharmacodynamics for volatile anaesthesia," *IEEE Trans. Biomed. Eng.*, vol. 61, no. 1, pp. 25–34, Jan. 2014.
- [14] C. M. Ionescu, I. Nascu, and R. Keyser, "Robustness tests of a model based predictive control strategy for depth of anaesthesia regulation in a propofol to bispectral index framework," in *International Conference on Advancements of Medicine and Health Care Through Technology*, vol. 36, S. Vlad and R. Ciupa, Eds. Berlin, Germany: Springer-Verlag, 2011, pp. 234–239.
- [15] I. Nascu, C. M. Ionescu, I. Nescu, and R. De Keyser, "Evaluation of three protocols for automatic DOA regulation using propofol and remifentanyl," in *Proc. Int. Conf. Control, Autom.*, 2011, pp. 573–578.
- [16] C. M. Ionescu, I. Nascu, and R. De Keyser, "Towards a multivariable model for controlling the depth of anaesthesia using propofol and Remifentanyl," in *Proc. 8th Symp. Biol., Med. Syst.*, 2012, pp. 325–330.
- [17] M. M. R. F. Struys, T. De Smet, S. Greenwald, A. R. Absalom, S. Bingé, and E. P. Mortier, "Performance evaluation of two published closed-loop control systems using bispectral index monitoring: A simulation study," *Anesthesiology*, vol. 100, pp. 640–647, 2004.
- [18] T. W. Schnider, C. F. Minto, P. L. Gambus, C. Andresen, D. B. Goodale, and S. L. Shafer, "The influence of method of administration and covariates on the pharmacokinetics of propofol in adult volunteers," *Anesthesiology*, vol. 88, pp. 1170–1182, 1998.
- [19] T. W. Schnider, C. F. Minto, S. L. Shafer, P. L. Gambus, C. Andresen, and D. B. Goodale, "The influence of age on propofol pharmacodynamics," *Anesthesiology*, vol. 90, pp. 1502–1516, 1999.
- [20] C. F. Minto, T. W. Schnider, and S. L. Shafer, "Pharmacokinetics and pharmacodynamics of remifentanyl—Part II: Model application," *Anesthesiology*, vol. 86, pp. 24–33, Jan. 1997.
- [21] C. F. Minto, T. W. Schnider, T. D. Egan, E. J. Youngs, H. J. Lemmens, and P. L. Gambus, "Influence of age and gender on the pharmacokinetics and pharmacodynamics of remifentanyl—Part I: Model development," *Anesthesiology*, vol. 86, pp. 10–23, 1997.
- [22] N. West, G. A. Dumont, K. Van Heusden, C. L. Petersen, S. Khosravi, and K. Soltesz, "Robust closed-loop control of induction and maintenance of propofol anaesthesia in children," *Paediatric Anaesthesia*, vol. 23, pp. 712–719, 2013.
- [23] C. S. Nunes, T. Mendonça, J. M. Lemos, and P. Amorim, "Feedforward adaptive control of the Bispectral Index of the EEG using the intravenous anaesthetic drug propofol," *Int. J. Adapt. Control Signal Process.*, vol. 23, pp. 485–503, 2009.
- [24] C. Ionescu, J. T. Machado, R. De Keyser, J. Decruyenaere, and M. M. R. F. Struys, "Nonlinear dynamics of the patient's response to drug effect during general anaesthesia," *Commun. Nonlinear Sci. Numer. Simul.*, vol. 20, pp. 914–926.
- [25] R. De Keyser, "Model Based Predictive Control," *Invited Chapter UNESCO Encyclopaedia Life Support Syst.*, vol. 6.43.16.1, p. 30p, 2003.
- [26] E. N. Pistikopoulos, M. Georgiadis, and V. Dua, *Multi-Parametric Programming: Theory, Algorithms and Applications*. Hoboken, NJ, USA: Wiley-VCH, 2007.
- [27] K. I. Kouramas, N. P. Faíscas, C. Panos, and E. N. Pistikopoulos, "Explicit/multi-parametric model predictive control (MPC) of linear discrete-time systems by dynamic and multi-parametric programming," *Automatica*, vol. 47, pp. 1638–1645, 2011.
- [28] (2010). P. S. E. L. (PSE). GPROMS model developer guide. Release v3.3.0 [Online]. Available: <http://www.psenterprise.com/gproms/>.
- [29] D. W. Clarke, C. Mohtadi, and P. Tuffs, "Generalized predictive control—Part I: The basic algorithm," *Automatica*, vol. 23, pp. 137–148, 1987.
- [30] C. Mohtadi, D. Clarke, and P. Tuffs, "Generalized predictive control—Part II: Extensions and Interpretations," *Automatica*, vol. 23, pp. 149–160, 1987.
- [31] G. F. Franklin, D. J. Powell, and A. Emami-Naeini, *Feedback Control of Dynamic Systems*. Englewood Cliffs, NJ, USA: Prentice-Hall, 2001.
- [32] E. N. Pistikopoulos, N. A. Bozinis, and V. Dua, "POP: A MATLAB implementation of multi-parametric quadratic programming algorithm," Centre for Process System Engineering, Imperial College, London, U.K., 1999.
- [33] G. Welch and G. Bishop, "An introduction to the Kalman filter: SIGGRAPH 2001 Course 8," in *Proc. Comput. Graph., Annu. Conf. Comput. Graph., Interact. Techn.*, 2001, pp. 12–17.
- [34] S. Yelneedi, L. Samavedham, and G. P. Rangaiah, "Advanced control strategies for the regulation of hypnosis with propofol," *Ind. Eng. Chem. Res.*, vol. 48, pp. 3880–3897, Apr. 15, 2009.

Authors' photographs and biographies not available at the time of publication.